PAPER

Polycyclic aromatic hydrocarbons in the soil profiles (0–100 cm) from the industrial district of a large open-pit coal mine, China

Xiaoyang Liu, [ID] [a] Zhongke Bai,*[ab] Qinfei Yu,*[cd] Yingui Cao[ab] and Wei Zhou[ab]

Mining and industrial activities are the primary sources of soil pollution in the open-pit coal mine. The concentrations of PAHs in 11 sampling sites in the industrial district and 9 sampling sites with different land use types in Pingshuo open-pit coal mine, China, were measured to investigate the distributions of PAHs and possible sources in soil profiles (0–100 cm). In the topsoil layer (0–20 cm), concentrations of 16 PAHs ranged from 2.15 to 33.51 mg kg^{-1}, with a mean value of 11.93 mg kg^{-1}. PAHs were more variable in the middle soil layer (20–50 cm), ranging from 0.199 to 36.888 mg kg^{-1} with the average value of 9.21 mg kg^{-1}. Comparable extreme concentrations were detected from the samples in the subsoil layer (50–100 cm). Compared with those in topsoil, the average concentrations of the most individual PAH species were less in the middle soil and subsoil layers. The concentrations of most of the individual PAHs in the topsoil were higher than those in the middle soil and subsoil. Distribution patterns of PAHs in the three soil layers correlated well with each other. The high concentration hotspots were concentrated around the old coal washery, reaching about 30 mg kg^{-1}. The average concentrations of PAHs with different rings in the industrial district exceeded those in the other land use types. However, only the concentrations of 5-ring PAHs in topsoil showed difference with different land use types ($P < 0.05$). Diagnostic ratios and the total index showed that petroleum combustion was the main source of PAHs.

1. Introduction

Polycyclic aromatic hydrocarbons (PAHs) belong to a type of organic contaminants with ubiquitous presence and carcinogenic potential in the ecosystem. They mainly arise from the natural or artificial incomplete combustion or pyrolysis of organic material.[1–3] Moreover, soil plays as an important sink for them.[4] Their presence and concentrations in soils are greatly influenced by human encroachment.[5] Industry, agriculture, and transport activities are the sources of soil contaminants, and these directly or indirectly contaminate soil *via* atmosphere or water by adsorption and deposition in the soil. Among the sources, atmospheric deposition is viewed as the most common source of soil pollution.[6] Accumulation of PAHs in soil degrades the soil quality; moreover, it may lead to additional potential contamination of food chains and vegetables.[7,8] Because of their

adverse effects, such as high toxicity, mutagenicity, and carcinogenicity,[9] on human health, they are receiving extensive attention.

Knowledge about the distribution of PAHs in different soil layers and contaminant sources is critical to minimize the environmental risks. The US Environmental Protection Agency (EPA) has highlighted 16 unsubstituted PAHs as priority pollutants that need monitoring. Numerous investigations found that PAHs are widely distributed in the environmental media such as sediments,[10] agriculture soil,[11] urban soil,[12] roadside soil,[13,14] industry-affected soil,[15,16] dump sites,[17] and mine-impacted soil.[18–20] Soil pollution in the coal mine area is mainly ascribed to coal exploitation, processing, and utilization.[21] Mining-impacted soils and industrially impacted soils are among the poorly structured soils and generally abundant with a toxic substance such as PAHs.[22] Research on the PAHs in soil influenced by the sole factor of mining activity or industrial activity is abundant. However, soils affected by these two different activities were generally separately researched. Information about the cofactors of mining operations and industrial activities on the PAHs in soils is rare.

To address the knowledge of PAHs in industrial soils in coal mines, the objectives of this study were to (1) investigate the impact of open-pit coal mining and industrial operations on the concentrations of PAHs in the soil profiles, (2) identify the

[a]*School of Land Science and Technology, China University of Geosciences (Beijing), Beijing 100083, PR China. E-mail: liuxiaoyangsd@163.com; Baizk@cugb.edu.cn; yuqinfei2003@163.com; caoyingui1982@126.com; zhouw@cugb.edu.cn; Fax: +86 10 82321807; Tel: +86 10 82322182*

[b]*Key Laboratory of Land Consolidation and Rehabilitation, Ministry of Land and Resources, Beijing 100035, PR China*

[c]*Chinese Academy of Land & Resource Economics, Beijing 101149, PR China*

[d]*Guanghua School of Management, Peking University, Beijing 100871, PR China*

possible sources of PAHs, and (3) explore the patterns and distribution of PAHs in the vertical direction.

2. Material and methods

2.1 Study area

The research was conducted in the largest open-pit coal mine in China – Pingshuo coal mine, which is located in the northern Shanxi Province on the Loess Plateau. This region is characterized by the typical temperate arid to semi-arid continental monsoon climate, with the average annual temperature of 4.8–7.8 °C and average annual precipitation of 428.2–449.0 mm.[23] Chestnut soil and loessial soil are dominant there, and they are characterized by the low content of organic matter. Moreover, due to the poor ecosystem resistance ability, this district belongs to a typical fragile eco-environmental zone in the Loess Plateau.

The specific study object was the industrial district in the Pingshuo coal mine. Its industrial activities started during the 1980s, and its area gradually expanded to 4.37 km^2 with the growing production of coal. It was constructed along a valley and was surrounded by three dumps: Inner Dump, South Dump of Antaibao coal mine, and West dump of Anjialing. About 2 km away in the northeast direction, there is a huge mining pit that is in use and emits a lot of waste. The industrial area serves as a coal assistant processing site, and different function areas are distributed in it, *e.g.*, the fired power plant, explosives plant, oil depot, coal washery, service depot, administrative area, sewage treatment plant, and coal slime piles. The location and overview of the industrial district are shown in Fig. 1.

2.2 Soil sampling and sample extraction

Soils from 11 locations in the industrial district were obtained at three depths of 0–20 cm, 20–50 cm, and 50–100 cm in August 2013 (Fig. 1). Near each sampling location, two other soil profiles were dug, and soils at the same depths were obtained and thoroughly mixed with each other into a composite sample to produce a representative sample and reduce the random variation. To perform a comparison with PAHs in soils under different land use types, soils from the original landscape, dump, middle, and lower reaches of the industrial district were also obtained as references. The samples were air-dried at room temperature and crushed after removing stones and residual roots and then passed through a 100-mesh sieve. Then, the soil samples were stored in brown bottles and transported to the lab to be stored at −20 °C.

Then, 10 g soil sample, spiked with surrogates (naphthalene-D8, acenaphthene-D10, phenanthrene-D10, chrysene-D12, and perylene-D12) and mixed with 10 g anhydrous sodium sulfate, was Soxhlet-extracted for 24 h with 200 mL hexane/acetone (1 : 1 v/v). The extract of soil was concentrated to approximately 0.5 mL after solvent exchange with hexane and then cleaned by silica gel column chromatography (25 cm × 1 cm i.d). The glass chromatography column, fitted with a Teflon stopcock, was packed from the bottom to top with glass wool, 10 g activated silica, and 2 g anhydrous sodium sulfate. The first 25 mL of eluent was discarded, and the second fraction containing PAHs eluted with 35 mL of *n*-hexane/dichloromethane (3 : 2 v/v) was obtained. The eluate was concentrated to 1 mL and the solvent changed to isooctane and then further concentrated to 0.2 mL under a gentle stream of nitrogen prior to analysis.
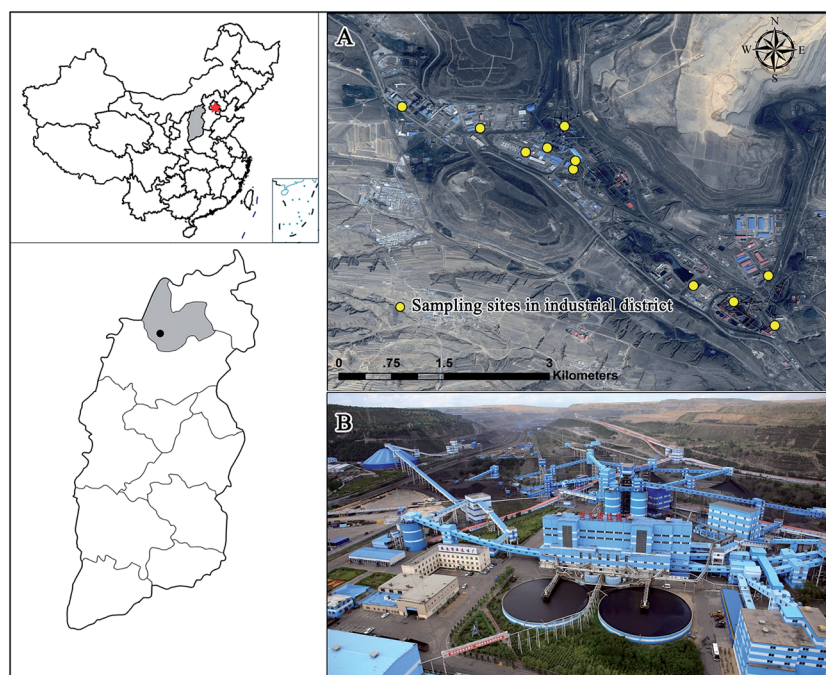

Fig. 1 Location of study area and soil sampling sites in the industrial district. (A) Sampling sites in the industrial district of Pingshuo open-pit coal mine and (B) overview of the industrial district.

2.3 Analytical methods and quality control

In all the soil samples, concentrations of 16 PAHs were determined: naphthalene (Nap), acenaphthylene (Acy), acenaphthene (Ace), fluorene (Fl), phenanthrene (Phe), anthracene (Ant), fluoranthene (Fla), pyrene (Pyr), benzo[*a*]anthracene (BaA), chrysene (Chr), benzo[*b*]fluoranthene (BbF), benzo[*k*]fluoranthene (BkF), benzo[*a*]pyrene (BaP), indeno[1,2,3-*cd*]pyrene (InP), dibenzo[*a,h*]anthrancene (DahA), and benzo[*g,h,i*]perylene (BghiP). PAHs were analyzed using an Agilent 6890 gas chromatograph-5975 mass selective detector (GC-MS) system equipped with a DB-5 column (30 m × 0.25 mm i.d., 0.25 μm film thickness). The chromatographic conditions were as follows: injector temperature 270 °C; detector temperature 280 °C; oven temperature initially at 60 °C for 5 min, increased to 290 °C at 3 °C min^{-1}, and maintained for 40 min. The detailed description of the analytical procedure for the measurement of PAHs has been described by Yang *et al.*[24] The detection limits of PAHs were 0.005 mg kg^{-1} (Table 1). The recovery efficiency was tested by analyzing soil samples spiked with a known amount of PAH standard, and the recoveries were found to be ranging from 80% to 98% for PAHs in the soil samples. A procedural blank analysis was performed with every 3 samples to monitor interferences and cross-contamination. All the samples were analyzed in triplicate, and errors were between ±10% and ±15% analytically.

2.4 Data analysis and mapping

All the concentrations of PAHs in this study were expressed on the basis of dry weight. The statistical significance was determined by an analysis of variance (ANOVA), and the significance level was established at $p < 0.05$. The inverse distance weighted (IDW) interpolation method was used to map the distributions of PAHs. The concentration of the individual PAHs, whose level

was below the detection limit, was considered as one-half of that limit.

3. Results and discussion

3.1 Concentrations of PAHs in the soil samples

The summary statistics including the minimum, maximum, mean, and standard deviation of 16 PAHs in three soil layers of the soil profiles (0–100 cm) are listed in Table 1.

In the topsoil layer (0–20 cm), concentrations of 16 PAHs ranged from 2.16 to 33.52 mg kg^{-1}, with a mean value of 11.94 mg kg^{-1}, much higher than that reported in agricultural soils,[25,26] urban soils,[27] coal and coal gangue,[28] whereas slightly lower than the concentrations of flue dust in a Hg and As mining and metallurgy brownfield.[29] The 7 probable human carcinogenic PAHs (including BaA, Chry, BbF, BkF, BaP, DahA, and InP) ranged from 1.09 mg kg^{-1} to 16.47 mg kg^{-1}, which was much higher than that in the soils around the Anhui coal district, China,[30] and even higher than that of the highly industrialized chemical/petrochemical area.[31] The average concentrations of Pyr and BbF were higher and similar, all higher than 1.70 mg kg^{-1}. The average concentration of Ace was the minima in 16 PAHs, with the value of 0.02 mg kg^{-1}. Pyr concentrations varied the most, ranging from 0.22 to 7.57 mg kg^{-1}, reflecting its labile characteristics in topsoil. At all the sites, Acy and Fl were not detected from the soil profiles. This is because they indicate recent deposition, and their decomposition is very quick, amounting to even 50% over a month.[32]

Compared with the topsoil layer, concentrations of 16 PAHs and 7 PAHs in the middle soil layer (20–50 cm) were more variable. Their values ranged from 0.23 to 36.90 mg kg^{-1} and 0.04 to 19.21 mg kg^{-1}, indicating heterogeneous levels of contamination in the middle soil. However, the average value (4.59) of 7 PAHs in the middle soil layer was lower than that in the topsoil layer (5.88). Among the individual PAHs, Phe was the

Table 1 Summary statistics for PAH concentrations (mg kg^{-1}) in soil profiles (0–100 cm) from the industrial district

Compound	MDL	Detection rate	0–20 cm				20–50 cm				50–100 cm			
			Min	Max	Mean	SD	Min	Max	Mean	SD	Min	Max	Mean	SD
Nap	5×10^{-3}	72.73%	2.5×10^{-3}	1.31	0.34	0.39	0.05	2.65	0.48	0.81	0.03	0.57	0.32	0.53
Acy	5×10^{-3}	0%	—	—			—	—			—	—		
Ace	5×10^{-3}	15.15%	2.5×10^{-3}	0.09	0.02	0.04	0.03	0.03	0.005	0.01	0.04	0.04	0.01	0.02
Fl	5×10^{-3}	0%	—	—			—	—			—	—		
Phe	5×10^{-3}	93.94%	2.5×10^{-3}	5.21	1.56	1.41	0.07	6.39	1.61	2.16	0.11	6.00	1.53	1.87
Ant	5×10^{-3}	78.79%	2.5×10^{-3}	0.92	0.23	0.26	0.02	0.76	0.16	0.24	0.02	0.85	0.18	0.25
Fla	5×10^{-3}	90.91%	2.5×10^{-3}	3.31	1.07	0.92	0.04	3.33	0.71	1.06	0.02	3.55	0.79	0.10
Pyr	5×10^{-3}	87.88%	2.5×10^{-3}	7.57	1.77	2.18	0.04	3.95	0.79	1.22	0.05	4.08	1.07	1.63
BaA	5×10^{-3}	24.24%	2.5×10^{-3}	2.86	0.47	0.92	0.88	3.05	0.52	1.01	1.01	3.08	0.45	0.93
Chr	5×10^{-3}	90.91%	2.5×10^{-3}	2.56	0.98	0.72	0.02	2.78	0.59	0.88	0.03	2.77	0.69	0.81
BbF	5×10^{-3}	87.88%	2.5×10^{-3}	4.50	1.75	1.13	0.17	5.03	1.20	1.54	0.13	5.32	1.29	1.43
BkF	5×10^{-3}	87.88%	2.5×10^{-3}	1.78	0.79	0.58	0.06	2.08	0.49	0.64	0.05	2.48	0.55	0.66
Bap	5×10^{-3}	66.67%	2.5×10^{-3}	2.39	0.93	0.67	0.15	3.03	0.65	0.96	0.34	2.76	0.67	0.82
InP	5×10^{-3}	78.79%	2.5×10^{-3}	1.93	0.83	0.54	0.13	2.65	0.62	0.79	0.06	2.27	0.62	0.68
DahA	5×10^{-3}	45.45%	2.5×10^{-3}	0.45	0.13	0.15	0.05	4.73	0.53	1.41	0.05	0.51	0.25	0.82
BghiP	5×10^{-3}	78.79%	2.5×10^{-3}	2.60	1.07	0.82	0.04	3.62	0.87	1.11	0.09	3.05	0.83	0.95
$\sum$7 PAHs			1.09	16.47	5.88	4.32	0.04	19.21	4.59	5.93	—	19.19	3.06	5.67
$\sum$16 PAHs			2.16	33.52	11.94	8.70	0.23	36.90	9.21	11.16	0.06	36.46	6.59	10.62

most abundant species, with the average concentration of 1.88 mg kg^{-1}. Apart from the difference in the minimum concentrations of 7 PAHs, comparable extreme concentrations of 16 PAHs and 7 PAHs were detected from the samples in the subsoil layer (50–100 cm) and middle soil layer. Phe was also the most abundant species in the subsoil layer, with the mean concentration of 1.53 mg kg^{-1}, similar to that in topsoil and middle soil. Compared with the samples in topsoil, average concentrations of the most individual PAH species were lower in the middle soil layer and subsoil layer, implying the relatively lower contamination of PAHs in a deeper soil depth.

According to the criteria reported in the previous study,[33] PAHs in soils could be divided into four groups based upon the concentrations: non-contaminated (<0.2 mg kg^{-1}), weakly contaminated (0.2–0.6 mg kg^{-1}), contaminated (0.6–1.0 mg kg^{-1}), and heavily contaminated (>1.0 mg kg^{-1}). According to this classification, all the samples in topsoil, 9 of 11 samples in middle soil, and 6 of 11 samples in subsoil were heavily contaminated.

3.2 PAH patterns

The congener patterns in 11 sample sites from different soil layers are shown in Fig. 2. The predominant PAHs were Phe and BbF for most samples in the profiles.

In the topsoil layer, Phe was the dominant constituent in the 2–3-ring PAHs and accounted for 15.55, 12.89, and 28.51% of a total of 16 PAHs at the sites I4, I7, and I9, respectively. BbF, similarly, occupied the highest proportion of the high molecular weight PAHs (5–6 rings) and accounted for 16.56, 15.00, 14.94, 16.96, 18.28, and 16.63% of a total of 16 PAHs at the sites I1, I2, I3, I6, I9, and I10, respectively. It was in line with the previous study results indicating that Phe and Bbf were among the predominant contributors of PAHs.[34,35] All the samples appeared to be dominantly affected by the high molecular weight 5- to 6-ring PAHs (5–6 ring PAHs = 34.02–58.14%). Concentrations of low molecular weight (2- to 3-ring) PAHs were low and only contributed 15.01–37.99% to the total PAHs, with one sample (I8) undetected, which may be due to its highly volatile character.[36]

In the middle soil layer, Phe accounted for 15.18%, 33.17%, and 53.36% of a total of 16 PAHs at the sites I2, I6 and I8, respectively. BbF accounted for 19.14%, 13.64%, 15.49%, 14.32%, and 20.24% of a total of 16 PAHs at the sites I1, I4, I5, I10, and I11, respectively. The high molecular weight PAHs were also the most abundant in the samples, except for the I8 sample in the middle soil layer, in which low molecular weight 2- and 3-ring PAHs accounted for 22.13% and 53.36%, respectively.

A similar trend was observed in the subsoil layer, which is an indicator of similar origin. Phe accounted for 48.26%, 18.37%, 22.05%, 89.19%, and 21.05% of a total of 16 PAHs at the sites I1, I2, I7, I8 and I9, respectively. BbF accounted for 14.59%, 17.78%, and 15.85% of a total of 16 PAHs at the sites I4, I5 and I6, respectively. Except for the site I8, samples primarily contained 5–6 ring PAHs than 2-ring PAHs. At site I10, 4 ring PAHs, as the sole detectable ring PAHs, contributed 100% to the total PAHs. The elevated percentage of 4-ring PAHs at this site may
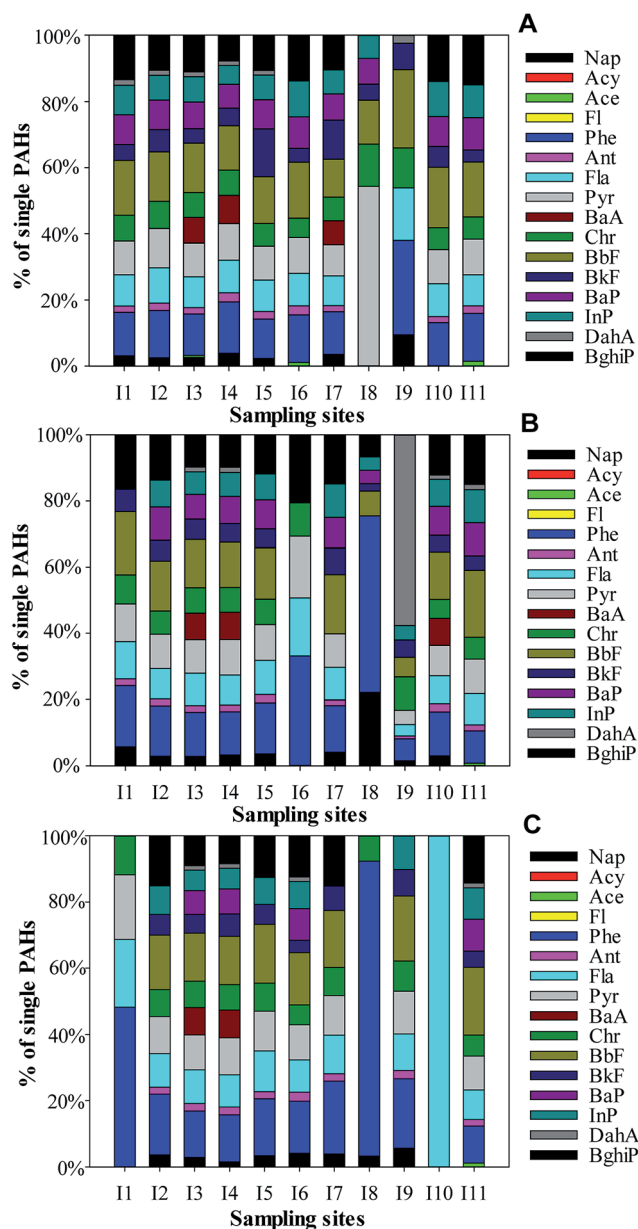
Fig. 2 Distribution of single compounds in the soil samples. (A) Sampling sites at 0–20 cm depth; (B) sampling sites at 20–50 cm depth; and (C) sampling sites at 50–100 cm depth.

arise from the coal-fired power plant in the immediate vicinity.[37] The distributions of the individual PAHs at sites I7 and I8 differed from those at other sites because their locations were near the oil depot and old coal washery, respectively. The contaminants emitted from the oil depot and old coal washery may exert a great effect on the PAH patterns.

3.3 Distributions of PAHs in horizontal and vertical directions

To analyze the mobility of PAHs in the vertical direction, the corresponding individual PAH concentrations of two different soil layers were divided as the concentration ratio (CR). The outcomes are depicted in Fig. 3. The ratio distributions among
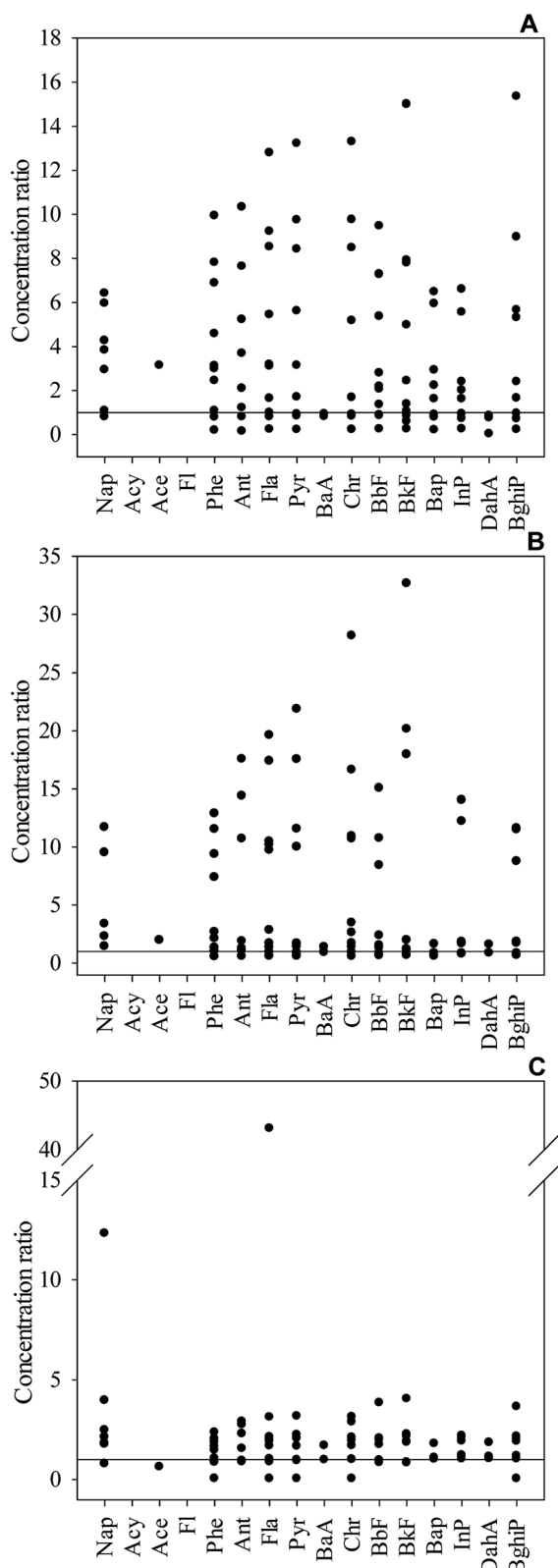
Fig. 3 Concentration ratios of PAHs in different soil layers in the industrial district. (A) Concentration ratio of 0–20 cm depth *vs.* 20–50 cm depth; (B) concentration ratio of 0–20 cm depth *vs.* 50–100 cm depth; and (C) concentration ratio of 20–50 cm depth *vs.* 50–100 cm depth.

different soil layers for 16 individual PAHs were variable, but they had a similar pattern, with most sites exceeding 1, which implied that PAH concentrations decreased with the increasing depth in the profile (0–100 cm). It was consistent with the earlier study.[38]

PAHs tend to accumulate in the topsoil because its strong sorption towards soil organic matter (SOM) and any other absorbing materials.[39] Most of the individual PAH concentrations in the topsoil were higher than those in the middle soil layer (Fig. 3A), apart from BaA and DahA. The percentage of ratios higher than 1 ranged from 55.56% (Chr) to 100% (Ace), illustrating the accumulation of PAHs in topsoil.[38]

The similar CR distributions (0–20 cm depth *vs.* 50–100 cm depth) for the individual PAHs were found and compared with those of 0–20 cm depth *vs.* 20–50 cm depth, with most ratios surpassing 1, except for BaA, DahA, and Bap, suggesting that the concentrations of PAHs in topsoil were higher than those in the subsoil layer. However, there were some sites in the middle soil and subsoil layers that had the concentrations of PAHs lower than those in the topsoil. It may arise from the disturbed soil with more contaminated material with elevated PAH concentrations reaching greater depths. Pies *et al.*[40] also found similar results in the coal-impacted soils.

Except for Fla at site I10 and NaP at site I8, the CRs were less variable for 20–50 cm depth *vs.* 50–100 cm depth, and most sites were concentrated between 0 and 5, evidenced that decrease in rate slowed down with the increasing soil depth.

Different physicochemical characteristics of PAHs affect their distribution in the atmosphere and soil.[41] To recognize the distribution of PAHs in different functional areas within the industrial district of the Pingshuo coal mine, IDW was applied to map and assess the spatial feature of 16 PAHs. The IDW interpolation maps of different soil layers are presented in Fig. 4.

According to the previous studies, PAH concentrations varied widely in different areas or different land use types due to the diverse contributors.[42,43] In this study, distribution patterns of PAHs in the three soil layers correlated well. The high concentration hotspots were concentrated around the old coal washery, reaching about 30 mg kg^{-1}. Around the fired power plant and explosives plant, PAH concentrations were relatively low: <8 mg kg^{-1} in the topsoil, <5 mg kg^{-1} in the subsoil, and 8–11 mg kg^{-1} in the middle soil. PAH concentrations near the service depot (e and j), administrative area (f and i), and new coal washery were low in middle soil and subsoil, lower than that in the corresponding areas of topsoil. PAHs are transferred to the soil *via* deposition.[44] Some studies suggested that higher molecular weight PAHs tend to deposit near the point of emission.[45,46] This may be one reason for the different PAH distributions in various function areas. Moreover, service time also has a significant influence on PAHs in soils; *e.g.*, soils near the new coal washery (k) in the soil profile showed PAH concentrations lower than that near the old coal washery (d).

3.4 Comparisons of PAH concentrations among different land use types

To compare the differences of PAH concentrations between the various land use types in the profile, the average and standard
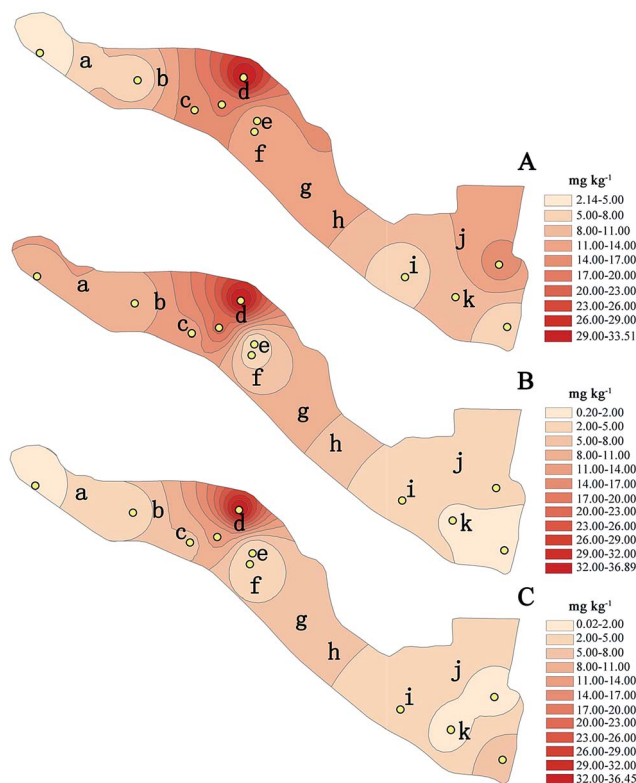
Fig. 4 Spatial distribution of $\sum$16 PAHs in different soil layers in the industrial district: (A) at 0−20 cm depth; (B) at 50−100 cm depth; and (C) at 50−100 cm depth. (a)−(f) represent the functional areas: (a) fired power plant, (b) explosives plant, (c) oil depot, (d) old coal washery, (e) service depot, (f) administrative area, (g) sewage treatment plant, (h) coal slime piles, (i) administrative area, (j) service depot, and (k) new coal washery.

Fig. 5 Comparison of PAH concentration of soils in the industrial district with soils in the original landscape, dump, and the middle and lower reaches. (A) Sampling sites at 0−20 cm depth; (B) sampling sites at 20−50 cm depth; and (C) sampling sites at 50−100 cm depth.

deviation at each site of the industrial district, original landscape, dump, and middle and lower reaches of the industrial area are summarized in Fig. 5.

The average concentrations of 2-ring to 6-ring PAHs and 16 PAHs of the topsoil in the industrial district were relatively higher than those of other land use types (Fig. 5A). Roberto et al.[47] also found that most PAHs have higher average concentrations in soils obtained from the industrial areas among all the sites. However, tested by one-way AVOVA, only 5-ring PAH concentrations showed a significant difference between different land use types at the 0.05 level. Similarly, average PAH concentrations of the middle soil and subsoil in the industrial district exceeded those in other land use types; however, their differences were not significant ($P < 0.05$).

The large proportion of high molecular weight parent PAHs in soils is a typical symbol of combustion origin.[48,49] Medium and high molecular weight PAHs seemed to be the most dominant in different land use types, especially the 4-ring and 5-ring PAHs, indicating that PAHs possibly originated from nearby resources, and it is also consistent with previous studies.[50,51] The vertical distribution patterns of the concentrations of PAHs varied in different land use types; e.g., PAH concentrations showed a decreasing trend with the increasing
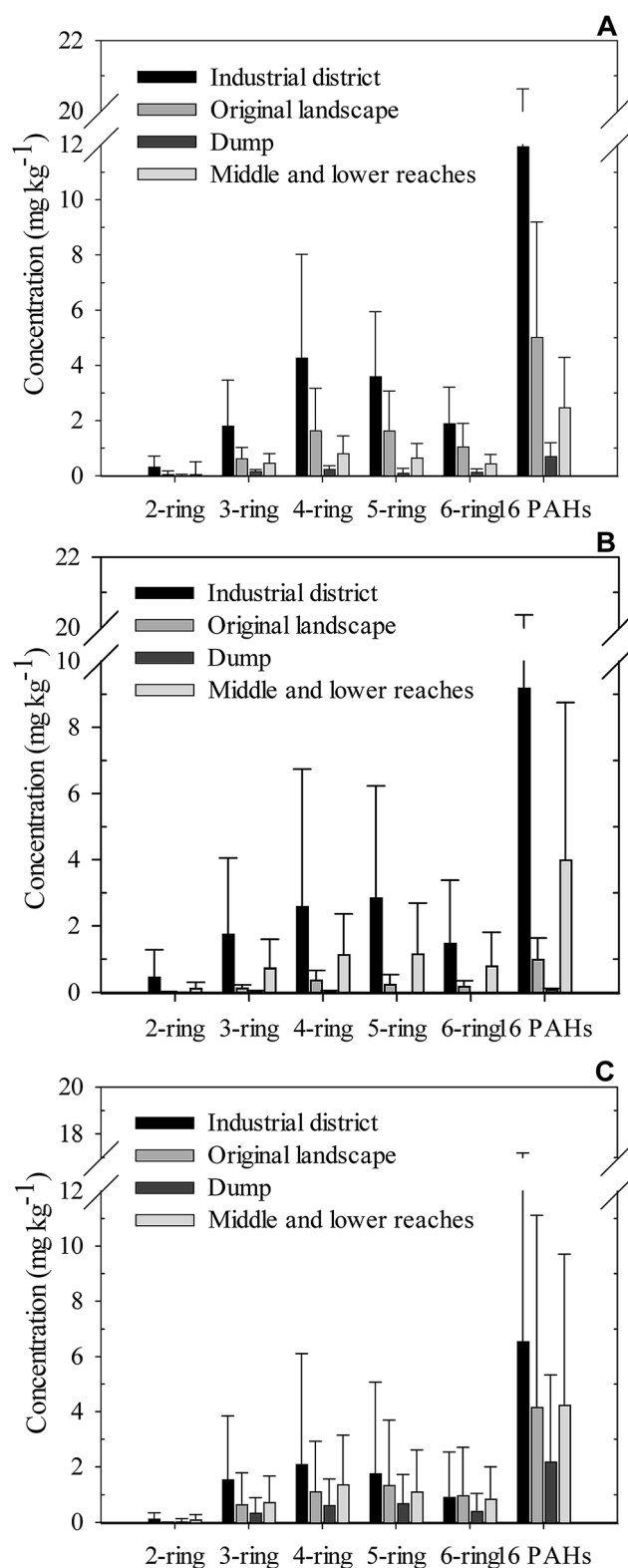
depth; PAH concentration of the middle soils seemed to be lower than that in the topsoil and subsoil of the original landscape and dump; PAH concentrations showed no difference between different soil layers in the middle and lower reaches. The dissimilar profiles may due to the different conditions of total organic carbon (TOC) values, vegetation coverage, plant species, and other organisms, which greatly influenced the diffusion of PAHs.[52–55]

3.5 Possible sources of PAHs

The relationships among Fla, Pyr, Ant, and Phe, as well as InP, BghiP, BaA, and Chr, are commonly used as reliable approaches to detect the possible PAH sources:[56–59] *e.g.*, the ratio of Fla/(Fla + Pyr) lower than 0.4 is characteristic of a petroleum source; greater than 0.5 implies combustion of coal, straw, and wood; and 0.4–0.5 characterizes petroleum combustion;[60] the Ant/(Phe + Ant) ratios less than 0.1 usually indicate petrogenic input, and a ratio greater than 0.1 implies a dominance of combustion.[61] A plot of the ratios between InP/(InP + BaP) *vs.* BaA/(BaA + Chr) and Ant/(Phe + Ant) *vs.* Fla/(Fla + Pyr) is given in Fig. 6. In this study, 83% of soil samples varied between the values of 0.4 < Fla/(Fla + Pyr) ratio < 0.5 and Ant/(Phe + Ant) ratio > 0.1 (Fig. 6A), implying a dominance of petroleum combustion effects in the industrial district,[48] which was also indicated by the plot of InP/(InP + BghiP) *vs.* BaA/(BaA + Chr). There were also other sources

in this area, but their contributions were relatively smaller. According to Fig. 6, PAH concentrations at the site I8 near the oil depot and site I6 near the coal washery indicated petroleum input. The highest value was found at site I10, indicating that the input of PAHs in the topsoil near the fired power plant was derived from coal combustion.

In some cases, the results concluded from the ratio values may differ from each other. Considering this, Santino Orecchio and Maria Rosaria Mannino[62,63] used a total index as the sum of single indices to distinguish between the low temperature sources and high temperature sources: total index = Fl/(Fl + Pyr)/0.4 + Ant/(Ant + Phe)/0.1 + BaA/(BaA + Chr)/0.2 + InP/(InP + BghiP)/0.2. If the total index is >4, high temperature processes (combustion) are generally considered as the PAH sources; otherwise, the low temperature processes (petroleum product) are viewed as the main sources of PAHs. Based on this theory, we calculated the total index for each soil sample in the industrial district and found that the total index for 87.88% of the samples exceeded 4, indicating that high temperature processes (petroleum product) were the main contributors of PAHs.

Petroleum has been widely used in industrial activities and transportation; thus, it was not an exception in this study area. It is also well known that vehicles and construction equipment emit large amounts of PAHs.[64] Based on the abovementioned analysis, we suggested that the excessive consumption of petroleum was the main contributors of PAHs in this area. Moreover, petroleum input and coal combustion also contribute to the elevated PAH concentrations in some functional areas.

4. Conclusion

Most of the soil samples at the depth of 0–100 cm in the industrial district were heavily contaminated by PAHs, and its concentrations were higher than those in soils from the original landscape, dumps, and middle and lower reaches. The spatial distribution and vertical distribution of PAHs in soils supported the hypothesis that PAHs tend to concentrate in topsoil and widely varied in different functional sub-areas. Medium and high molecular weight PAHs seemed to be the most dominant in different land use types, especially the 4-ring and 5-ring PAHs. Although the PAH sources were complex in this area, analysis of diagnostic ratios and total index indicated that petroleum combustion was the most significant contributor. PAH inputs from coal combustion were relatively small.

There are numerous coal workers working and living in the industrial district. The high PAH concentrations in soils may pose a risk to their health, and the health protection measures are worth noting. Control of oil consumption in industry and mining activities and replacement with cleaner energy may reduce the soil pollution caused by PAHs, especially that of the HMW species.
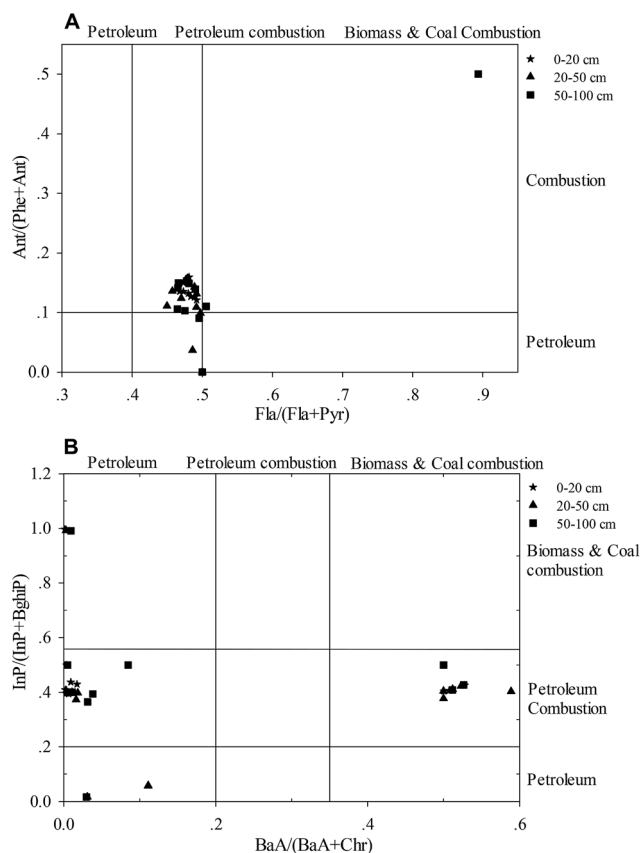

Fig. 6 Cross-plot for the isomeric ratio of InP/(InP + BaP) *vs.* BaA/(BaA + Chr) and Ant/(Phe + Ant) *vs.* Fla/(Fla + Pyr) in the soil profiles of the industrial district.

Acknowledgements

Yang, Xingding Hu and Xiaorong Kou for their help with the field and laboratory work. We are extremely grateful to the anonymous reviewers for their insightful comments and suggestions.

References

1 S. Orecchio, *J. Hazard. Mater.*, 2010, **180**, 590–601.
2 A. Cachada, P. Pato, T. Rocha-Santos, E. F. Da Silva and A. C. Duarte, *Sci. Total Environ.*, 2012, **430**, 184–192.
3 S. Orecchio, D. Amorello, S. Barreca and A. Valenti, *Microchem. J.*, 2016, **124**, 267–271.
4 T. Agarwal, P. S. Khillare, V. Shridhar and S. Ray, *J. Hazard. Mater.*, 2009, **163**, 1033–1039.
5 Z. Z. Ouyang, L. M. Gao, X. Q. Chen, S. P. Yao and S. H. Deng, *RSC Adv.*, 2016, **6**, 71441–71449.
6 X. D. Li, C. S. Poon and P. S. Liu, *Appl. Geochem.*, 2001, **16**, 1361–1368.
7 A. M. Kipopoulou, E. Manoli and C. Samara, *Environ. Pollut.*, 1999, **106**, 369–380.
8 S. Orecchio, *Atmos. Environ.*, 2007, **41**, 8669–8680.
9 Y. F. Jiang, X. T. Wang, M. H. Wu, G. Y. Sheng and J. M. Fu, *Environ. Monit. Assess.*, 2011, **183**, 139–150.
10 S. Orecchio, F. Bianchini, R. Bonsignore, P. Blandino, S. Barreca and D. Amorello, *Polycyclic Aromat. Compd.*, 2016, **36**, 429–451.
11 J. Jefimova, J. Adamson, J. Reinik and N. Irha, *Environ. Sci. Pollut. Res.*, 2016, **23**, 20862–20870.
12 X. S. Wang, *Environ. Earth Sci.*, 2013, **70**, 2855–2864.
13 D. K. Essumang, K. Kowalski and E. G. Sogaard, *Bull. Environ. Contam. Toxicol.*, 2011, **86**, 438–443.
14 M. Saeedi, L. Y. Li and M. Salmanzadeh, *J. Hazard. Mater.*, 2012, **227–228**, 9–17.
15 D. Wu, Y. L. Wang, W. J. Liu, Y. C. Chen, X. F. Fu, S. Tao and W. X. Liu, *Environ. Sci.*, 2016, **37**, 740–749.
16 J. Wang, X. F. Zhang, W. T. Ling, R. Liu, J. Liu, F. X. Kang and Y. Z. Gao, *Chemosphere*, 2017, **168**, 976–987.
17 A. Subramanian, T. Kunisue and S. Tanabe, *Chemosphere*, 2015, **137**, 122–134.
18 J. Nawab, S. Khan, M. Aamir, I. Shamshad, Z. Qamar, I. Din and Q. Huang, *Environ. Sci. Pollut. Res.*, 2016, **23**, 2381–2390.
19 N. N. Peng, Y. Li, Z. G. Liu, T. T. Liu and C. Gai, *Sci. Total Environ.*, 2016, **565**, 1201–1207.
20 E. V. Yakovleva, D. N. Gabov, V. A. Beznosikov, B. M. Kondratenok and Y. A. Dubrovskiy, *Polycyclic Aromat. Compd.*, 2016, 1–18.
21 Z. K. Bai, M. C. Fu and Z. Q. Zhao, *Ecology and Environment*, 2006, **15**, 1122–1125.
22 J. Nawab, S. Khan, M. T. Shah, Z. Qamar, I. Din, Q. Mahmood, N. Gul and Q. Huang, *Environ. Monit. Assess.*, 2015, **187**, 605.
23 X. Y. Liu, Z. K. Bai, W. Zhou, Y. G. Cao and G. J. Zhang, *Ecol. Eng.*, 2017, **98**, 228–239.
24 D. Yang, S. H. Qi, Y. Zhang, X. L. Xing, H. X. Liu, C. K. Qu, J. Liu and F. Li, *Mar. Pollut. Bull.*, 2013, **76**, 298–306.
25 J. J. Nam, B. H. Song, K. C. Eom, S. H. Lee and A. Smith, *Chemosphere*, 2003, **50**, 1281–1289.
26 W. Wilcke, *J. Plant Nutr. Soil Sci.*, 2000, **163**, 229–248.
27 M. Trapido, *Environ. Pollut.*, 1999, **105**, 67–74.
28 H. F. Huang, X. L. Xing, Z. Z. Zhang, S. H. Qi, D. Yang, D. A. Yuen, E. H. Sandy, A. G. Zhou and X. Q. Li, *Environ. Geochem. Hlth.*, 2016, **38**, 1169–1181.
29 J. R. Gallego, N. Esquinas, E. Rodriguez-Valdes, J. M. Menendez-Aguado and C. Sierra, *J. Hazard. Mater.*, 2015, **300**, 561–571.
30 R. W. Wang, G. J. Liu, C. L. Chou, J. J. Liu and J. M. Zhang, *Arch. Environ. Contam. Toxicol.*, 2010, **59**, 62–70.
31 M. Nadal, M. Schuhmacher and J. L. Domingo, *Chemosphere*, 2007, **66**, 267–276.
32 P. Oleszczuk and S. Baran, *Pol. J. Environ. Stud.*, 2003, **12**, 431–437.
33 B. Maliszewska-Kordybach, *Appl. Geochem.*, 1996, **11**, 121–127.
34 J. Ma and Y. Z. Zhou, *J. Environ. Sci.*, 2011, **23**, 1518–1523.
35 C. Lors, D. Damidot, J. Ponge and F. Perie, *Environ. Pollut.*, 2012, **165**, 11–17.
36 E. Morillo, A. S. Romero, C. Maqueda, L. Madrid, F. Ajmone-Marsan, H. Grcman, C. M. Davidson, A. S. Hursthouse and J. Villaverde, *J. Environ. Monit.*, 2007, **9**, 1001–1008.
37 A. Arditsoglou, C. Petaloti, E. Terzi, M. Sofoniou and C. Samara, *Sci. Total Environ.*, 2004, **323**, 153–167.
38 B. A. M. Bandowe, N. Shukurov, M. Kersten and W. Wilcke, *Environ. Pollut.*, 2010, **158**, 2888–2899.
39 G. Cornelissen, O. Gustafsson, T. D. Bucheli, M. Jonker, A. A. Koelmans and P. Van Noort, *Environ. Sci. Technol.*, 2005, **39**, 6881–6895.
40 C. Pies, B. Hoffmann, J. Petrowsky, Y. Yang, T. A. Ternes and T. Hofmann, *Chemosphere*, 2008, **72**, 1594–1601.
41 R. Iturbe, R. M. Flores and L. G. Torres, *Environ. Geol.*, 2003, **44**, 608–620.
42 K. Y. Wang, Y. T. Shen, S. C. Zhang, Y. B. Ye, Q. Shen, J. D. Hu and X. J. Wang, *Environ. Geol.*, 2009, **56**, 1041–1050.
43 Y. Wang, Z. J. Tian, H. L. Zhu, Z. N. Cheng, M. L. Kang, C. L. Luo, J. Li and G. Zhang, *Sci. Total Environ.*, 2012, **439**, 187–193.
44 N. B. Vogt, F. Brakstad, K. Thrane, S. Nordenson, J. Krane, E. Aamot, K. Kolset, K. Esbensen and E. Steinnes, *Environ. Sci. Technol.*, 1987, **21**, 35–44.
45 S. Y. N. Yang, D. W. Connell, D. W. Hawker and S. I. Kayal, *Sci. Total Environ.*, 1991, **102**, 229–240.
46 A. Motelay-Massei, D. Ollivon, B. Garban and M. Chevreuil, *Atmos. Environ.*, 2003, **37**, 3135–3146.
47 J. Roberto, W. Y. Lee and S. I. Campos-Díaz, *J. Hazard. Mater.*, 2009, **163**, 946–958.
48 H. Budzinski, I. Jones, J. Bellocq, C. Pierard and P. Garrigues, *Mar. Chem.*, 1997, **58**, 85–97.
49 L. F. Ping, Y. M. Luo, H. B. Zhang, Q. B. Li and L. H. Wu, *Environ. Pollut.*, 2007, **147**, 358–365.
50 V. Kapsimalis, I. P. Panagiotopoulos, P. Talagani, I. Hatzianestis, H. Kaberi, G. Rousakis, T. D. Kanellopoulos and G. A. Hatiris, *Mar. Pollut. Bull.*, 2014, **80**, 312–324.
51 H. Kwon and S. Choi, *Sci. Total Environ.*, 2014, **470**, 1494–1501.

52 B. W. Bogan, W. R. Sullivan, K. H. Cruz, J. R. Paterek, P. I. Ravikovitch and A. V. Neimark, *Environ. Sci. Technol.*, 2003, **37**, 5168–5174.

53 R. Vácha, J. Čechmánková and J. Skála, *Plant, Soil Environ.*, 2010, **56**, 434–443.

54 Y. Wang, C. L. Luo, J. Li, H. Yin, X. D. Li and G. Zhang, *Chemosphere*, 2011, **85**, 344–350.

55 R. A. Kanaly and S. Harayama, *J. Bacteriol.*, 2000, **182**, 2059–2067.

56 W. Wang, M. J. Huang, Y. Kang, H. S. Wang, A. O. W. Leung, K. C. Cheung and M. H. Wong, *Sci. Total Environ.*, 2011, **409**, 4519–4527.

57 J. Li, Y. Huang, R. Ye, G. L. Yuan, H. Z. Wu, P. Han and S. Fu, *J. Geochem. Explor.*, 2015, **158**, 177–185.

58 B. Yu, D. Zhang, L. H. Tan, S. P. Zhao, J. W. Wang, L. Yao and W. Cao, *RSC Adv.*, 2017, **7**, 4671–4680.

59 S. Suman, A. Sinha and A. Tarafdar, *Sci. Total Environ.*, 2016, **545**, 353–360.

60 M. B. Yunker, R. W. Macdonald, R. Vingarzan, R. H. Mitchell, D. Goyette and S. Sylvestre, *Org. Geochem.*, 2002, **33**, 489–515.

61 L. Z. Zhu, Y. Y. Chen and R. B. Zhou, *J. Hazard. Mater.*, 2008, **150**, 308–316.

62 S. Orecchio, *J. Hazard. Mater.*, 2010, **173**, 358–368.

63 M. R. Mannino and S. Orecchio, *Atmos. Environ.*, 2008, **42**, 1801–1817.

64 G. Lammel, J. Klanova, J. Kohoutek, R. Prokes, L. Ries and A. Stohl, *Environ. Pollut.*, 2009, **157**, 3264–3271.